Power Quality Enrichment and Power Management using an Adaptive Control Scheme in Microgrid System

Narendra Babu P[†], Non-member

ABSTRACT

This article proposes an ANFIS-based control scheme for improved power quality and power management that will provide optimal and sustainable energy in a grid-connected renewable energy system. The system consists of a wind energy conversion system (WECS), a photo voltaic system (PVS), and a battery energy storage system (BESS). To increase the PVS's and WECS output powers, a unique control approach is suggested in this paper. The adaptive Neuro-Fuzzy Inference System (ANFIS) controller is incorporated into the proposed controller to generate three-phase reference current signals for harmonic elimination in the system during system dynamic conditions. The proposed control technique can work under voltage quality problems such as voltage sag, voltage swell, neutral currents, and reactive power. Renewable energy sources (PV and Wind) are interfaced to improve the DC-link overall performance by minimizing short-term and long-term voltage problems. The proposed controller regulates the energy flows between the renewable energy sources to the end users with a unity power factor. A supervisory control scheme is implemented for optimal power management in the system. Based on the load requirement, how the renewable, battery, and grid sources are sharing the power, a detailed analysis is given in the paper. Simulation results from the MATLAB/Simulink platform under several test conditions at the grid side and load side are illustrating the efficacy of the proposed control mechanisms in the environment of power optimization and energy management. The comparative analysis is performed to show the efficacy of the proposed system. Finally, the proposed system is validated and the THD content of the grid currents is found good.

Keywords: PLL, Wind Conversion System (WECS), Battery Energy Storage System (BESS), Isolated Hybrid Power System (IHPS), MPPT, PMDC, PCC

Manuscript received on April 8, 2024; revised on June 14, 2024; accepted on August 6, 2024. This paper was recommended by Associate Editor Chainarin Ekkaravarodome.

The author is with School of EEE, VIT Bhopal University, Kothrikalan, Bhopal-Indore Highway, Sehore, MP-466114, India.

[†]Corresponding author: narendrababup204@gmail.com

Digital Object Identifier: 10.37936/ecti-eec.2024223.253559

1. INTRODUCTION

Everybody's existence now revolves around energy. We can no longer imagine a world without energy. Everyone needs the energy to complete daily tasks like operating a computer, operating a phone, or cooking meals. All these activities require energy to operate, With the advancement of technology, energy consumption is rising quickly. A man's everyday needs start consuming energy in a variety of ways from the first minute of the day until the very last. Many people today find it difficult to imagine a world without energy. therefore, serves as the foundation for both the development of a country and the existence of an individual [1].

Hybrid renewable energy systems are already gaining popularity for use in outlying areas where grid power is impractical. To achieve an effective energy supply in remote places, several renewable energy technologies, such as solar systems and mini-grids, have been implemented. When they are first introduced, many of them, typically because there aren't enough sales to cover the costs of replacing the product and operating and maintaining it, give real creativity to the end user or aren't even practicable [2]. The news is already spreading among all system investors due to the expansion of the global grid, and there is a worry that when the grid arrives at a specific region, it will offer useless off-grid systems. Apart from that, with the increase in GHG emissions in recent years, climate change has become a major environmental concern. It has become necessary to come up with alternative energy resources that can produce electricity. Hence, solar energy and wind energy have become good alternatives for producing affordable electricity [3].

A few years ago, power was only produced via solar energy. During overcast or stormy days, only solar energy systems can produce their full amount of power. Solar system users won't have a source of electricity until the battery is fully empty. As a consequence, the power can be increased by integrating the processes for producing solar and wind energy. The quiet and pollution-free running of electric power generation systems is ensured by these integrated technologies. The seasonal nature of the autonomous systems prevents them from acting as reliable energy sources. One can utilize a hybrid system that employs both solar and wind energy to build a balanced approach to energy production and to gain from the advantages of each system while also overcoming its drawbacks. It may be feasible to lower the cost of power

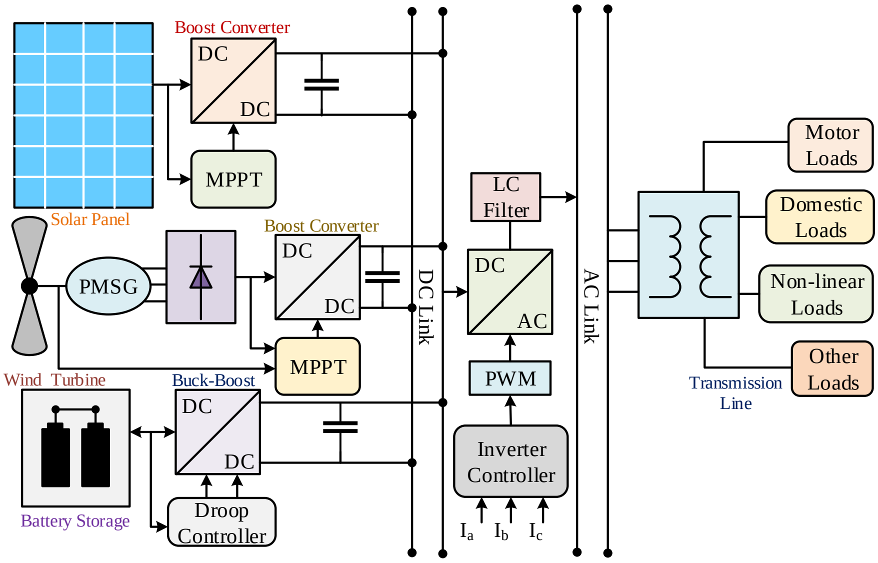

***Fig. 1**: Schematic for grid-tied hybrid PV-wind-battery system with interfaced active power filter and potential control strategy.*

per unit because the amount of solar and wind energy obtained varies by region, but this cannot be guaranteed.

This article investigates a system that provides consistent performance at a low cost [4-5]. The depletion of fossil resources and the rising need for electricity has dominated global relations for the decade preceding. As a result, Renewable Energy Sources (RES) have been created from unrestricted, universally accessible, environmentally friendly natural resources like solar radiation, wind speed, tides, and waves. From a technological and financial standpoint, the effective deployment of RES is increasingly appropriate to provide power in such remote locations. One RES or a hybrid RES can be used to establish electricity in remote places. Due to their complementarity, solar photovoltaic and wind energy sources are the most popular combinations employed in RES. On the other extreme, the Hybrid Renewable Energy System (HRES) can be complemented by extra energy sources (such as a motor or storage system) to ensure a steady supply of electricity if the RES fails to deliver sufficient power [6].

The major figure in a functioning standalone HRES is being able to supply the user with the energy they require despite the substantial variations in RES power output caused by changes in weather conditions while maintaining the frequency and voltage supplied to consumers within reasonable parameters. This work, which is now being presented, suggests control solutions to address this issue and increase power quality while increasing the IHPS's cost-effectiveness and reliability. As aware, there are numerous different off-grid systems and their core concepts, including hydro-energy, geothermal energy, and others. Improving power supply reliability has been the subject of numerous tests over the past few years, but the results have not been encouraging. These trials failed primarily because many participants could not afford the significant energy costs involved in the tests.
So, the system discussed in this article is built on several optimization algorithms that will improve the system's capacity, deliver consistent power at lower costs, and lessen people's financial stress [7]. This hybrid power generating system, which combines solar and wind energy, will reduce the induced power instability in variable renewable energy systems while also improving the system's overall capability and trustworthiness. The device's capability for quantity utilization might be decreased, which would severely reduce costs. Active power filters (APFs) and their control strategies are a valid choice for reducing harmonics and enhancing the quality of electricity in grid-tied systems. Exactly how well the APF performs depends on the configuration of grid-interfacing inverters, dc voltage, etc. A DC-Link controller is generally used to calculate the switching losses of inverters and the production of the reference current. These days, there are many ways to control DC buses, including sliding mode fuzzy logic control and fuzzy logic control [8-9]. It is anticipated that loads will suddenly connect and be removed from the distribution line. The existence of nonlinear loads at the load side has a major impact on the grid's power quality. To maintain system performance, which is directly related to power quality, conditioners such as active power filters, passive power filters, and hybrid active power filters have been evaluated and found to be effective. Thus, the power system's concerns with voltage quality and rising current are widespread yet need attention. Hence, shunt active power filters are used to address current quality concerns, while series active power filters are employed to address voltage quality difficulties. The grid-connected PV system with current quality improvements has been the focus of research. The grid's demand for high-quality voltage has not gone unnoticed. There

have been numerous reports of literature reviews for various types of voltage quality improvement strategies [10]. The control mechanisms' function is crucial in creating the right switching signals for the compensator's converters. The injecting signal for the distribution lines is established with the aid of these switching signals. Because of how simple and effective the PID controller's implementation is, it is a common control strategy used in industrial operations. Moreover, gain parameters (k_p,k_i, and k_d), which are difficult to calculate, affect the controller's performance.

There are a number of detrimental effects of increased harmonics in the power system, such as external heat, harmonic amplification caused by banks of power factor correction capacitors, reduced transmission system efficiency, overheated power transformers, malfunctioning electronic components, ineffective circuit breaker operation, measurement error generation, and interference with communication and control signals. Numerous industries, including business, healthcare, and aviation, are harmed by poor power quality. Even in health care contexts, it can have disastrous effects and impair vital interactions. When a nation's electricity is of poor quality, it hurts its economy since it reduces overall production [11]. PQ problem-solving techniques have received a lot of attention, including active filters (AF), passive filters (PF), hybrid filters (HF), and specialised power devices. A PF is a practical, affordable, and reasonable solution to harmonic-related issues in the electrical power supply. The size, resonance, complexity of the filter design, and tuning difficulties of PFs are some of their drawbacks. Recent studies have shown that active filtering approaches for PQ augmentation outperform passive methods in terms of reaction times, size, and performance. By actively responding to changes in network parameters, active filtering also reduces the likelihood of resonance between the filter and the network impedance. The drawbacks of the separate active and passive filtering operations are removed by a hybrid power filter (HPF), which combines the functions of PFs and an active power filter(APF) [12]. Although there are many HSAPF controllers available in the literature, they are only effective for a small number of problems. Conventional controllers struggle to fix some persistent system flaws. Fuzzy logic and neural networks are used as controllers to improve system performance. A controller implementation to provide harmonic compensating voltage is made by the Adaptive Neuro-fuzzy Inference System (ANFIS). Given that the system's load fluctuates, the reference current computations must be performed simultaneously. This article mentions an ANFIS-based digital processor generates PWM signals for switching components in the SAPF and gating signals for thyristors in the adaptive shunt passive filter. The redesigned P-Q controller serves as the principal controller for regulating the active and reactive power characteristics. The voltage profile of the system can be improved using ANFIS. For the active filter to satisfy the nonlinear load's requirements for reactive and harmonic power, it must deliver the necessary compensation signals.

In the literature, grid interfacing inverter control schemes have been implemented to control power quality, power factor, active and reactive power in the cited works. Fryze theories [8] and reactive power (IRP) [9], synchronous reference frame (SRF) [10], improved IRP [11], improved SRF [12], Instantaneous symmetrical component (ISC) etc. [13] are the few conventional control schemes for power quality improvement in the microgrid. However, the behavior of the control scheme is unacceptable during dynamic grid and load conditions. Moreover, the traditional control schemes are not suitable for grid-synchronization, FC extraction, and both voltage and current harmonic elimination [8-13]. To overcome these constraints, numerous adaptable control schemes have been developed in the cited works such as least mean square (LMS) [14], normalized LMS (NLMS)[15], leaky LMS (LLMS) [16], Hebbian LMS (HLMS) [17], modified LMS (MLMS) [18], variable step size LMS (VSS-LMS) [19], least mean fourth (LMF) [20], unbiased circular leakage centered (UCLC) [21], least mean mixed-norm (LMMN) [22], echo state network (ESN) [23], robust normalized Mixed-Norm (RNMN) [24]. However, these control techniques exhibit poor dynamic behavior under unbalanced loads and varying loads. Moreover, the LMF scheme has a poor convergence rate due to its fourth-order optimization, which impacts the steady-state performance of the system [14-28].

Our model has made the following significant contributions:

1. A hybrid and efficient power management and power quality improvement system that combines solar and wind energy is included in this article.
2. The goal of this paper is to identify a solution to the issues provided by the grid-connected system, such as zero carbon emissions, power management and improved power efficiency, with a particular emphasis on the system's energy costs.
3. The proposed system comprises fuzzy and neural networks that can enhance system performance. This paper also employs a controller known as the Adaptive Neuro-fuzzy Inference System (ANFIS) to generate the harmonic compensation in the system.
4. This system consists of a supervisory controller that controls the power flow from the IHPS to continuously supply load demand even in the face of changing weather.
5. The system is operated under several grid and load dynamic conditions to check the efficacy of the controller. In all the test cases, the controller performed well.
6. When the grid is under abnormal circumstances, the model will function better compared to the other control schemes.
7. In comparison to traditional methodologies, the proposed control scheme provides improved filtering

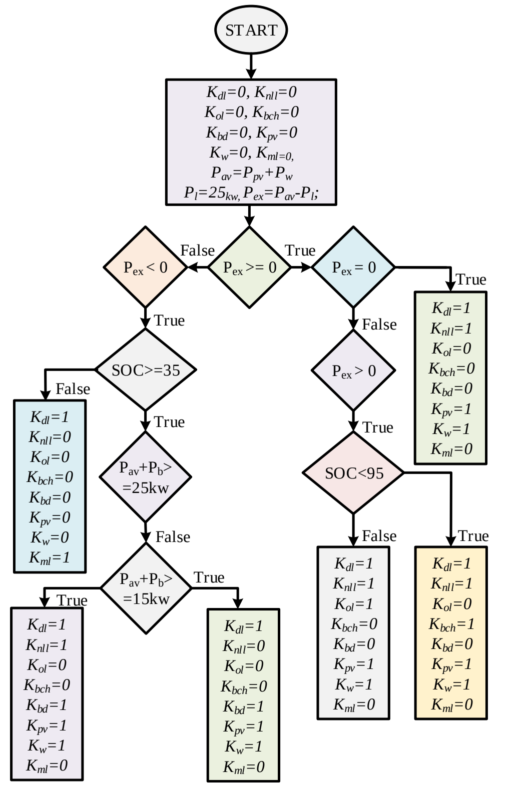

Fig. 2: *Schematic for Energy Management system for IHPS.*

capabilities. Also, it is more dependable, versatile and find better performance in several characteristics.

2. SYSTEM DESCRIPTION

An original MPPT controller and a PV array make up the PVS. The boost converter's duty cycle can be altered to boost the PV system's output power. A variable-speed wind turbine (WT), a PMSG, an uncontrolled AC-DC diode bridge rectifier, and a stage of DC-DC conversion for MPPT made up of a boost converter controlled by a maximum power point tracking technique to squeeze the most power out of the WT by modulating the duty cycle make up the WECS. Energy storage systems (ESS) are used to store extra energy from RESs and make up for power shortages during power outages. The ESS is made up of a battery bank and a bidirectional DC-DC buck-boost converter coupled to the DC bus to maintain the DC bus voltage constant at the proper level despite the power variations between the RES and loads. A PWM VSI reverses the constant DC voltage that is obtained from the two RES systems and the ESS before sending the sinusoidal current to the AC load through an LC filter. A motor load is connected to the AC bus system to directly supply the home loads when the total quantity of energy required is more than the amount of energy supplied by the RES and batteries. A supervisor was created in this article to monitor the electrical supply to the loads and the power flows between the IHPS devices.

3. ENERGY MANAGEMENT SYSTEM FOR IHPS

By managing the power flow of the IHPS, the supervisory controller is primarily responsible for maintaining load fulfilment, particularly in the face of erratic weather. The provided energy management algorithm decreases the use of batteries and ML while relying mostly on energy generated by the PVS and WECS to satisfy demand, thereby increasing fuel efficiency and safeguarding the environment.

Four inputs are used,comprising the power measured P_{pv} and P_w from the PVS and WECS, the power required by loads, and the battery bank SOC. Seven contactor control signals are produced by the management controller: K_{pv} of the PVS, K_w of the WECS, K_{bd} of the battery discharging, K_{bch} of the battery charging, K_{dl} of the Domestic loads, K_{nll} of the Non-linear loads, K_{ol} of the other loads and K_{ml} of the Motor loads.

3.1 PVS Model

P-N junctions made from semiconductor materials with various doping levels make up solar cells. In this way, a straightforward circuit made up of a current source can display the solar cell. The nonlinear impedance of the p-n junction was once represented by a diode D in conjunction with a diode, IPH stands for the cell photocurrent, while r_S and r_{SH} stand for series and shunt resistance, accordingly. The following equations can be used to numerically represent the cell's output current, i_{SC}:

$$i_{SC} = i_{PH} - i_{SH}\cdot\left(exp\left(\frac{Q.(V_{out} + r_S.i_{SC})}{\omega.k.t}\right) - 1\right) - \frac{V_{out} + r_S.i_{SC}}{r_{SH}} \quad (1)$$

Where; i_{SC}: Solar Cell Current(A), V_{out}: Solar Cell Output Voltage(V), i_{PH}: Solar Generated Current(A), i_{SH}: Diode Saturation Current(A), r_s: Solar Cell Series Resistance(Ω), r_{SH}: Solar Cell Shunts Resistance(Ω), ω: Ideality Factor, t: Cell Temperature in Kelvin(K), k: Boltzmann Constant.

The voltage-current and power-current nonlinear characteristics of the PV cell are mostly dependent on temperature and insolation. On the panels, PV cells are connected in series and parallel circuits to produce the desired high power. To produce a PV generator (PVG), these modules can also be reorganised and connected in series and/or parallel. The PVG model with $m_s \times m_p$ cells is represented as follows using the PV cell model:

$$i_{pvG} = m_p.i_{PH} - m_p.i_{SH}\cdot\left(exp\left(\frac{Q.(Z_{pvG} + r_{SG}.i_{pvG})}{m_s.\omega.k.t}\right) - 1\right) - \frac{Z_{pvG} + r_{SG}.i_{pvG}}{r_{SHG}} \quad (2)$$

Where m_s and m_p are the numbers of parallelly and serially connected PV cells, respectively.

3.2 Wind Turbine Model

The mechanical power output that the wind turbine extracts is stated as follows:

$$W_m = \frac{1}{2}.C_P.\sigma.s_w.u_w^3 \tag{3}$$

Where; W_m: Mechanical Power, s_w: Wind Turbine Rotor Swept Area(m^2), u_w: Wind Speed(m/s), σ: AirDensity(kg/m^3), C_P: Power Coefficient.

The coefficient C_P is regarded as a crucial parameter in power regulation. It represents the proportion of mechanical power to wind power. Each type of turbine has its own non-linear C_P function. In this study, the power coefficient is defined as a function of the tip speed ratio ζ and the blade pitch angle θ, respectively:

$$C_P(\zeta,\theta) = C_1\left(\frac{C_2}{\zeta_i} - C_3\theta - C_4\right).e^{-\frac{C_5}{\zeta_i}} + C_6.\zeta \tag{4}$$

Where C_1 to C_6 are the power coefficients. The ratio between the speed of a wind turbine's blade tips and the speed of the wind ζ is known as the "tip speed ratio."

$$\zeta = \frac{\varpi_m R}{u_w} \tag{5}$$

Where: ϖ_m is the mechanical angular velocity of the generator (rad/sec) and R is the rotor's radius(m).

3.3 PMSG Model

The Park's (d, q) system can be used to express the dynamic model of PMSG as, [?]

$$\begin{aligned}\begin{bmatrix}V_d\\V_q\end{bmatrix} = -\begin{bmatrix}r_{st} & 0\\0 & r_{st}\end{bmatrix}\begin{bmatrix}i_d\\i_q\end{bmatrix} - \begin{bmatrix}G_d & 0\\0 & G_q\end{bmatrix}\frac{\mathrm{d}}{\mathrm{dt}}\begin{bmatrix}i_d\\i_q\end{bmatrix}\\ - u_e\begin{bmatrix}0 & -G_q\\G_d & 0\end{bmatrix}\begin{bmatrix}i_d\\i_q\end{bmatrix} + u_e\begin{bmatrix}0\\\varphi_m\end{bmatrix}\end{aligned} \tag{6}$$

Where; r_{st}: Stator Resistance, G_d and G_q: Inductances of the generator, φ_m: Permanent Magnet Flux and u_e: Electrical Rotating Speed of the Generator, defined by:

$$u_e = p \times u_m \tag{7}$$

Where p is the total number of generator pole pairs. As shown by, the electromagnetic torque equation,

$$C_{em} = \frac{3}{2}p\left\{(G_d - G_q)i_d i_q - \varphi_m i_q\right\} \tag{8}$$

The voltage across inductors is used to indicate the power, inductor (L_a), and capacitor (C) provided current (i_p) accumulated in the inductor as,

$$yV_a = L_a * \frac{di_p}{dt}. \tag{9}$$

The following expression can be used to determine the boost converter's inductor value:

$$L = \frac{V_{in} * D_T * t}{\Delta i} \tag{10}$$

Where Δi is the inductor ripple current, V_{in} is the input voltage, D_T is the duty cycle, and t is the time period.

$$V_{out} = \frac{V_{in}}{1 - D_T} \tag{11}$$

To improve wind energy output, a buck-boost converter is coupled to PMSG using MPPT methods. The following formula represents the line-line voltage of the Rms value's maximum output voltage of V_m.

$$V_{Rms} = \frac{\sqrt{3}V_m}{\sqrt{2}}. \tag{12}$$

After rectification, the voltage is represented by when the buck-boost converter steps up or down.

$$V_{DC} = \frac{D_T}{1 - D_T} * V_{DC\,Ry} \tag{13}$$

The power management monitoring algorithm uses the following scenarios as a summary:

1. 25 kW of power is produced overall by PVS and WECS. The Domestic and Non-linear loads will only be met by RESs in this circumstance.
2. If the energy from RES is greater than the energy needed by the load and the SOC is below 95%, the extra energy is used to charge the batteries.
3. The supervisory controller connects the other loads if the energy from RES is greater than the load demand and the SOC is not less than 95%.
4. To power loads, wind and solar energy are insufficient. In this case, the RES and batteries will power the domestic and non-linear loads if the SOC is higher than 35% and the total generation power from the sources exceeds 25 kW.
5. In the case that the combined output of the RES and batteries is only 15 kW, the supervisory controller disconnects the non-linear loads and solely supplies the domestic loads.
6. When the SOC is less than 35% and the load cannot be supplied by PV or wind energy sources, a Motor load turns on to provide only the Domestic loads.

4. PROPOSED CONTROL STRUCTURE

4.1 Conventional Controller

Instantaneous data can be used to demonstrate the p-q theory for three-phase power systems with or without neutrals. Along with the typical voltage and current waveforms, it also covers waveforms in steady state and transient conditions.

The a-b-c coordinates are translated to the α -β - 0 reference frame using Clark's transformation, which is the foundation of the p-q theory, a method for figuring

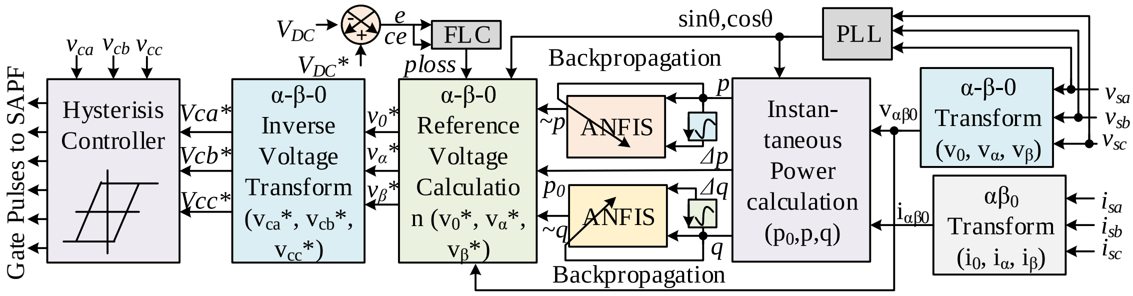

Fig. 3: ANFIS-based Controller for reference current signal generation.

out the current and voltage components of a three-phase input voltage. To determine the instantaneous reference voltages for the SAPF, a simplified p-q theory is needed. The source voltages are rotated by 90 degrees in modified p-q theory to determine instantaneous reactive power. Rather than employing the conventional AC components to create the compensating reference voltage, LPFs, and inverse transformations are applied to eliminate the DC components from the reference voltage.

As shown in Figure 3, the main objective of the control is to determine a three-phase reference compensation current (I^*_{ca}, I^*_{cb} and I^*_{cc}, respectively). This current will be used to account for distortions in the supply phase voltage (v_{sa}, v_{sb}, and v_{sc}, respectively) at the load terminals by injecting compensating currents (i_{ca}, i_{cb}, and i_{cc}, respectively) in the appropriate way so as to achieve full sinusoidal at PCC. The optimum voltages at the load terminals are the supply voltage and the injected SAPF voltage. To lessen the distortion of the supply voltage, phase-locked loops (PLL), which synchronize with the supply voltage, are employed. Voltage measurements on three phases are picked up and supplied into a PLL, which generates unit vectors for the ($\sin\omega t$, $\cos\omega t$) quadrature functions. When the PLL receives the measured voltages from the supplies, it will have a gain value that is appropriate. PLLs with independent three-phase modes provide a frequency of 50 Hz at 50 milliseconds. The properties of the three-phase supply voltages v_α, v_β, and v_0 and the three-phase source currents i_α, i_β, and i_0 make up the α-β-0 reference frame voltage and current. By eliminating the harmonic components of the voltage source, this filter helps to recover some of the genuine power that was lost in the crucial voltage component. This filter allows for the recovery of some of the actual power expressed. By reducing the harmonic components of the voltage source, this filter helps to recover part of the true power that was lost from the crucial voltage component.

The actual power is partially restored by this filter in the following ways:

$$\begin{bmatrix} V_0 \\ V_\alpha \\ V_\beta \end{bmatrix} = \sqrt{\frac{2}{3}} \begin{bmatrix} \frac{1}{\sqrt{2}} & \frac{1}{\sqrt{2}} & \frac{1}{\sqrt{2}} \\ 1 & -\frac{1}{\sqrt{2}} & -\frac{1}{\sqrt{2}} \\ 0 & \frac{\sqrt{3}}{2} & -\frac{\sqrt{3}}{2} \end{bmatrix} \begin{bmatrix} v_{sa} \\ v_{sb} \\ v_{sc} \end{bmatrix} \tag{14}$$

$$\begin{bmatrix} i_0 \\ i_\alpha \\ i_\beta \end{bmatrix} = \sqrt{\frac{2}{3}} \begin{bmatrix} \frac{1}{\sqrt{2}} & \frac{1}{\sqrt{2}} & \frac{1}{\sqrt{2}} \\ 1 & -\frac{1}{\sqrt{2}} & -\frac{1}{\sqrt{2}} \\ 0 & \frac{\sqrt{3}}{2} & -\frac{\sqrt{3}}{2} \end{bmatrix} \begin{bmatrix} i_{sa} \\ i_{sb} \\ i_{sc} \end{bmatrix} \tag{15}$$

In the α-β-0 reference frame, the compensating current, represented by $i^*_{c\alpha}$, $i^*_{c\beta}$ and i^*_{c0}, respectively, is expressed as,

$$\begin{bmatrix} i^*_{c\alpha} \\ i^*_{c\beta} \\ i^*_{c0} \end{bmatrix} = \frac{1}{i^2_\alpha + i^2_\beta} \begin{bmatrix} i_\alpha & i_\beta & 0 \\ i_\beta & -i_\alpha & 0 \\ 0 & 0 & i_{\alpha\beta} \end{bmatrix} \begin{bmatrix} \tilde{p} \\ \tilde{q} \\ p_0 \end{bmatrix} \tag{16}$$

where $\tilde{p}$ and $\tilde{q}$ are referred to as the alternating or variable elements and p and q are referred to as essential components. The reference currents I^*_{ca}, I^*_{cb} and I^*_{cc} in the reference frame are determined by multiplying the compensating voltage $i^*_{c\alpha}$, $i^*_{c\beta}$ and i^*_{c0} in the a-b-c reference frame with the expression as,

$$\begin{bmatrix} I^*_{ca} \\ I^*_{cb} \\ I^*_{cc} \end{bmatrix} = \sqrt{\frac{2}{3}} \begin{bmatrix} \frac{1}{\sqrt{2}} & 1 & 0 \\ \frac{1}{\sqrt{2}} & -\frac{1}{\sqrt{2}} & \frac{\sqrt{3}}{2} \\ \frac{1}{\sqrt{2}} & -\frac{1}{2} & -\frac{\sqrt{3}}{2} \end{bmatrix} \begin{bmatrix} i^*_{c\alpha} \\ i^*_{c\beta} \\ i^*_{c0} \end{bmatrix} \tag{17}$$

4.2 Proposed Controller

Figure 4 illustrates an example of an ANFIS structure, with a square denoting an adaptive node and a circle denoting a fixed node [6]. This graphic also includes hidden layers and input and output nodes. The fuzzy rules and membership functions are designed to handle the dynamic conditions in a microgrid [6].

$$p' = p(n) - \overline{p}(n), \tag{18}$$

$$q' = q(n) - \overline{q}(n), \tag{19}$$

$$f_1 = p_1 x + q_1 y + r_1, \tag{20}$$

$$f_2 = p_2 x + q_2 y + r_2, \tag{21}$$

$$f_3 = p_3 x + q_3 y + r_3, \tag{22}$$

$$f = \frac{W_1 f_1 + W_2 f_2 + W_3 f_3}{W_1 + W_2 + W_3} = \overline{W_1} f_1 + \overline{W_2} f_2 + \overline{W_3} f_3, \tag{23}$$

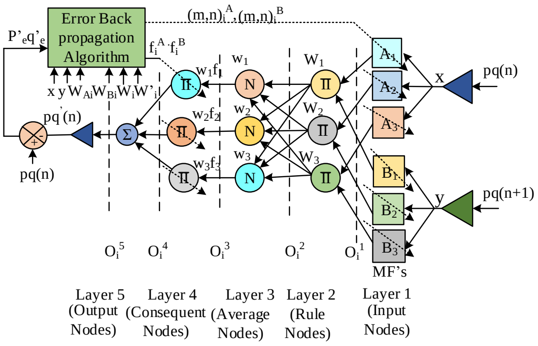

***Fig. 4**: Modified Architecture of ANFIS Controller.*

***Table 1**: Specification of system parameter*

Specifications	Simulation
PV power	2 kW
Wind power	1.7 kW
Wind speed	10m/s
Irradiations	1000 K/m^2
Grid Voltage	415 V
Frequency (f)	50 Hz
Source impedance	Rs=0.02Ω , Ls=1.3mH
DC voltage	700 V

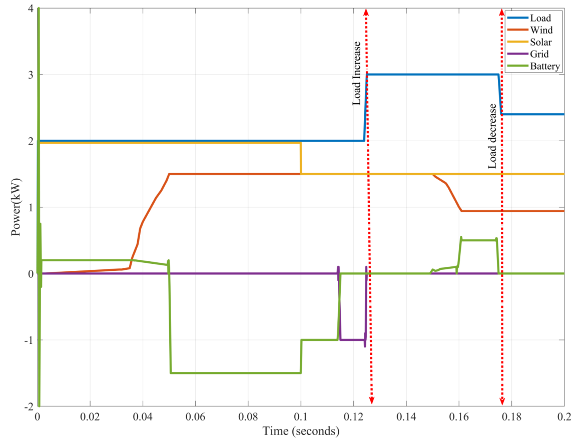

***Fig. 5**: case-1.*

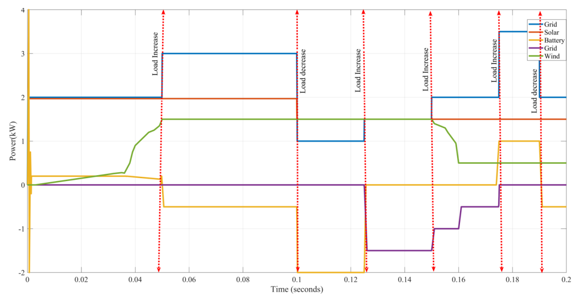

***Fig. 6**: case-2.*

5. RESULTS AND DISCUSSION

The complete system has been controlled using MATLAB and Simulink. Grid-tied PV, wind, and battery systems are used to apply the power quality enrichment technique in steady state, dynamic load, load removal, and unbalanced grid voltage scenarios. To regulate the HSAPF DC links through RES interfaces, a modified PQ theory implementation based on ANFIS is examined in this section. Using MATLAB and Simulink, the effectiveness of this control approach in various scenarios is evaluated.

5.1 Output results

In order to maintain power balance, Figure 5 shows a power management system (PMS) with a linked load of 2 kW and PV powering 2 kW simultaneously. 1.5 kW of power were produced by the wind at time t = 0.05. The remaining 1.5 kW will start to be stored in the batteries, as the load is currently only 2 kW.

The battery is needed because PV output decreases from 1.5 kW to 1 kW at time t = 0.1. The battery is fully charged at time t = 0.114; therefore, the PMS is sending 1 kW of power to the grid. At t = 0.125, the load has grown by 1 kW; at this time, the load is 3 kW; 1.5 kW of power is being supplied singly by the PV and the wind, leaving no net power; and the remaining kW is being supplied by the PV. At time t = 0.16, wind power decreases from 1.5 kW to 1 kW, adding up to the total.

Power is balanced at time t = 0.05 in Figure 6 when the wind starts to produce 1.5 kW of electricity and the load increases from 2 kW to 3 kW, resulting in an overall power production of 3.5 kW while we are only requiring 3 kW to 0.5 kW of power to charge the batteries.

At time t = 0.1, when the demand is dropped to 1 kW, the solar power output likewise drops to 1.5 kW, resulting in a 3 kW total power output. Only 1 kW of load will be used, so 2 kW will be used to charge the battery. The battery is fully charged when the load exceeds 1.5 kW at time t = 0.12, and the remaining 1.5 kW of power is sent to the grid. load at time t = 0.18.

As of time t = 0, Figure 7 depicts the connected load of 0.5 kW. At t = 0.05, when solar power increases to 1.5 kW and supplies 1 kW to the battery, PV is supplying 0.5 kW concurrently, balancing the power. A total power output of 2 kW is generated by the wind once it starts to generate 0.5 kW of electricity at time t = 0.06. 1.5 kW of power will be transferred to the battery, despite the fact that power usage is 0.5 kW. 0.5 kW of electricity will be delivered to the grid at time 0.07, when the load is 1.5 kW, the total power production is 2 kW, and the battery is fully charged. 1.5 kW of power will be sent to the grid when the load is 1.5 kW at time 0.10, the total power output is 2 kW, and the battery is completely charged.

At time t = 0, Figure 8 depicts a PMS with a 2 kW connected load.The electricity is balanced by PV, which is simultaneously producing 2kW. While both the load

***Table 2**: Individual Harmonics Analysis*

Conditions	3rd	5th	7th	9th	11th	13th	15th	17th	19th	21th	23th	25th	27th	29th	31th
Nonlinear sag and swell without control	7.2%	3.2%	3.3%	5.1%	1%	6.5%	4.1%	0.7%	0.3%	3.2%	2.5%	0.4%	1.2%	1%	0.6%
Nonlinear sag and swell with control	0.02%	0.1%	0.01%	0.01%	0.01%	0.01%	0.01%	0.01%	0.01%	0.01%	0.01%	0.01%	0.01%	0.01%	0.01%
Nonlinear without control	10.1%	5.7%	4%	3.1%	2.5%	2.1%	1.9%	1.6%	1.5%	1.3%	1.2%	1.1%	1%	1%	0.9%
Nonlinear with control	0.02%	0.01%	0.01%	0.01%	0.01%	0.01%	0.01%	0.01%	0.01%	0.01%	0.01%	0.01%	0.01%	0.01%	0.01%
dynamic with sag and swell without controller	6.5%	2.4%	1.4%	1.2%	0.8%	0.2%	0.8%	0.5%	0.4%	0.6%	0.2%	0.3%	0.3%	0.3%	0.3%
dynamic with sag and swell with controller	0.01%	1.8%	0.9%	0.01%	0.7%	0.5%	0.01%	0.4%	0.3%	0.01%	0.2%	0.2%	0.01%	0.2%	0.1%
dynamic without controller	10%	6.4%	4.3%	3.8%	2.6%	2.2%	1.9%	1.7%	1.6%	1.2%	1.3%	1.1%	1.1%	0.9%	0.9%
dynamic with controller	0%	1.8%	0.9%	0%	0.7%	0.5%	0%	0.4%	0.3%	0%	0.3%	0.2%	0%	0.2%	0.1%
single phase dynamic load without controller	7.7%	11%	5.4%	11%	5.1%	1.7%	2.5%	2.3%	3.4%	0.8%	1.3%	0.6%	1.2%	0.5%	1%
single phase dynamic load with controller	0.01%	1.8%	0.9%	0%	0.7%	0.5%	0%	0.4%	0.3%	0%	0.3%	0.2%	0%	0.2%	0.1%
single phase dynamic load sag and swell without controller	6.4%	2.4%	1.4%	1%	0.8%	0.6%	0.5%	0.5%	0.4%	0.4%	0.3%	0.3%	0.3%	0.3%	0.2%
single phase dynamic load sag and swell with controller	0.01%	0.01%	0%	0%	0%	0%	0.01%	0.01%	0%	0%	0%	0%	0%	0%	0%
single phase nonlinear without controller	10.3%	5.8%	4.1%	3.2%	2.5%	2.2%	1.9%	1.7%	1.5%	0.3%	1.2%	1.1%	1.1%	1%	0.8%
single phase nonlinear with controller	0.1%	0.2%	0.4%	0%	0.1%	0.1%	0.01%	0.1%	0.1%	0.01%	0.1%	0.1%	0.01%	0.1%	0.1%
single phase nonlinear sag and swell without controller	0.02%	22.6%	10.7%	0%	8.5%	5.7%	0%	4.7%	3.6%	0%	2.9%	2.3%	0.01%	1.9%	1.5%
single phase nonlinear sag and swell with controller	0.3%	0.2%	0.4%	0.1%	0.1%	0.1%	0.01%	0.1%	0.1%	0%	0.1%	0.1%	0.0%	0.1%	0.1%
Vl_Il_Is_without_battery_without controller	10.2%	6.3%	4.3%	3.9%	2.6%	2.2%	1.9%	1.7%	1.5%	1.2%	1.3%	1.1%	1.1%	0.9%	0.9%
Vl_Il_Is_without_battery_with controller	0%	1.8%	0.9%	0%	0.7%	0.5%	0%	0.1%	0.3%	0%	0.3%	0.2%	0%	0.2%	0.1%

***Table 3**: Comparative analysis of proposed control system*

Characteristics	Proposed	GSC-RC	FSVPWM	RSMES	RADRC	SFOC	FRT	ISOGI	GSC
PLL Used	Yes	Yes	No	Yes	Yes	Yes	Yes	Yes	Yes
Grid synchronization	Yes	Yes	No	Yes	Yes	Yes	Yes	Yes	Yes
THD	2.25%	3.4%	3.6%	3.3%	3.2%	4.0%	3.6%	3.2%	4.0%
Sampling Time	50μs	50μs	50μs	50μs	50μs	50μs	50μs	50μs	50μs
Accuracy	Better	Good	Good	Good	Good	Moderate	Moderate	Good	Moderate
Types Of Filter	Adaptive	Adaptive	Adaptive	Adaptive	Adaptive	Adaptive	Adaptive	Adaptive	Adaptive
Settling Time	0.04s	0.17s	0.03s	0.05s	0.20s	0.12s	0.9s	0.06s	0.10s
Amplitude tracking	Yes	Yes	Yes	No	No	No	No	Yes	No
Complexity	Less	Moderate	Moderate	Less	Moderate	Moderate	Less	Moderate	Moderate
DC offset rejection	Yes	No	No	No	No	No	Yes	No	No

***Table 4**: Comparative Analysis of the Proposed Control Technique with Conventional Control Techniques*

Characteristics	**Proposed**	**SRF**	**SRF-PLL**	**SPLL**	**ISRF**	**IRP**	**SCSRF**	**Adaline**	**SRF-VZ**	**LC-GCC**
Complicity	Less	Less	Medium	Medium	Less	Medium	Medium	Medium	Medium	Medium
THD of grid	2.13%	3.57%	2.64%	2.16%	2.84%	3.14%	2.94%	4.28%	2.21%	3.34%
FC evocation	Yes	No	Yes	Yes	No	No	No	No	No	No
Amplitude track	Yes	Yes	Yes	Yes	Yes	No	Yes	Yes	Yes	Yes
Cost	Low	Low	Medium	Medium	Medium	Medium	Medium	Medium	Medium	Medium
Clark's/park's Transf.	Yes	Yes	Yes	Yes	Yes	Yes	Yes	No	Yes	No
Sampling time	50μs	50μs	50μs	50μs	50μs	50μs	50μs	50μs	50μs	50μs
Precision	Better	Moderate	Good	Good	Modest	Modest	Modest	Modest	Good	Modest
PLL required	No	Yes	Yes	Yes	No	No	No	No	Yes	No
Filtering	Flexible	Flexible	Flexible	Flexible	Flexible	Flexible	Flexible	Flexible	Flexible	Flexible
Study-state break	0.023s	0.022s	0.025s	0.03s	0.025s	0.031s	0.027s	0.028s	0.19	0.015s

and the solar panel output drop to 1 kW at time t = 0.01, the load and solar panel output both rise to time t = 0.05 at time t = 0.022. Due to the low load power of 2 kW and the total production power of 2 kW (1.5 kW from the PV + 2 kW from the wind) = 3.5 kW, batteries will begin to store the 1.5 kW of excess electricity. Time t = 0.1 saw a reduction in battery power from 1.5 kW to 1 kW. The power management system is able to send 1 kW of electricity to the grid since the battery is fully charged at time t = 0.114. At time t = 0.125, the load increased by 1 kW, resulting in a combined output of 3 kW from the PV and wind sources.

5.2 Dynamic Load

In the figure below, a dynamic load is linked in this case at 0.1 seconds. The higher grid current shows that the grid is receiving power injection. Additionally, Figure 9 shows the control characteristics and makes the change in control characteristics clear. In this case, the suggested method yields a THD value of 28% for the harmonic content of the phase-A grid current. It is also looked at how effectively the PV-integrated ANFIS-based control system performs when the PCC voltage is subjected to sag and swell perturbations. For the sag and swell scenarios, we looked at a 10% increase and a 10% decrease in the nominal grid voltage.

5.3 Voltage Sag and Swell

The same period is shown in the figure below with a 75% voltage sag and no voltage injection during the time range of 0.12 and 0.16 seconds. The system's voltage peaks, troughs, and interruptions are all taken into consideration by the modified p-q theory control technique.

5.4 Load removed balanced Supply

In this instance, the voltage balance of a single-phase load interconnected between two phases is assessed. The voltage that was previously observed for compensation is used by the controller to determine the reference compensating voltage for the HC. Accurate identification

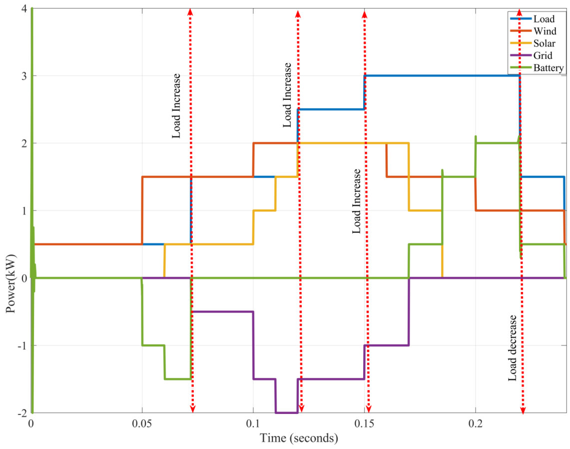

Fig. 7: *case-3.*

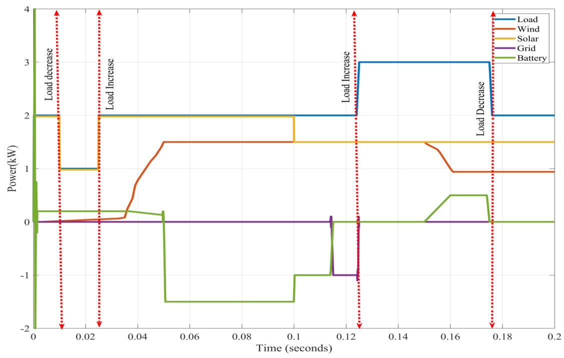

Fig. 8: *case-4.*

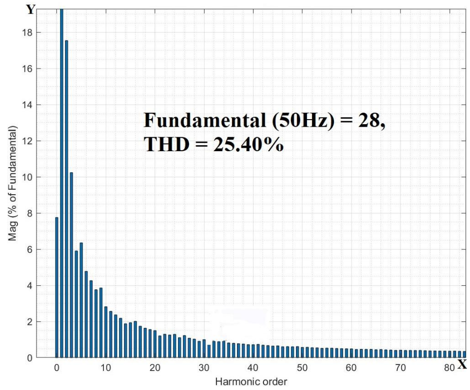

Fig. 10: *FFT analysis under dynamic without controller.*

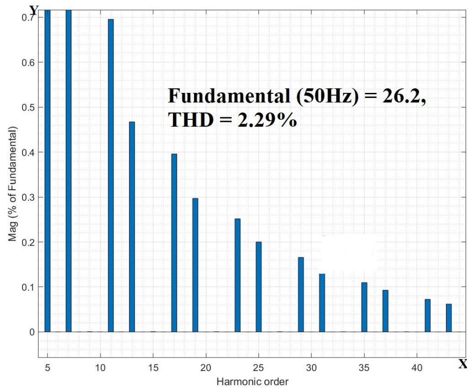

Fig. 11: *FFT analysis under dynamic with controller.*

of phase angle jumps and voltage imbalances is necessary to calculate the voltage and current injected through the SAPF.

5.5 Load Removed with Sag and Swell

The graphic shows that the THD value in this scenario with sag and swell disturbances is 28.11%. Figure 18 demonstrates how the regulating operation can lower THD by as much as 2.24 percent. The hysteresis controller uses the p-q model based on ANFIS to generate the required gating signal and calculates the required voltage for compensation. The modified p-q theory control approach for SAPF based on ANFIS eliminates voltage sag, voltage swell, and interruption by introducing a constant compensating voltage in series with the supply voltage at phase angles of 0° and 180. Due to the numerous harmonics that precede the adjustment, the suggested controller successfully modifies neutral currents. Before and after the adjustment, the THD values for three-phase source currents using the ANFIS controller are displayed. In this instance, the THD levels for three-phase source currents are taken into account both before and after the ANFIS controller modifications.

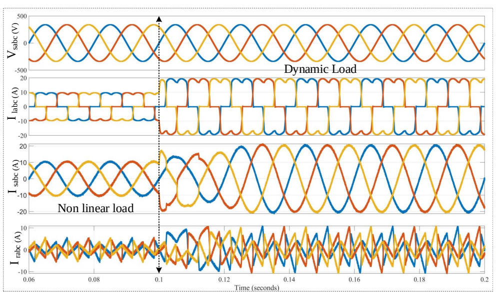

Fig. 9: *Dynamic load.*

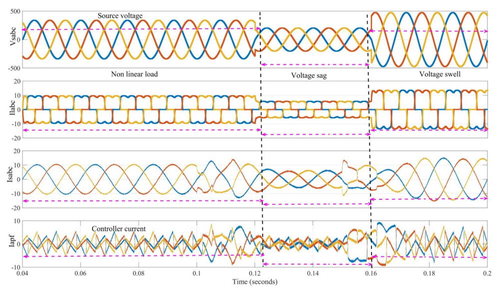

Fig. 12: *Voltage sag and swell.*

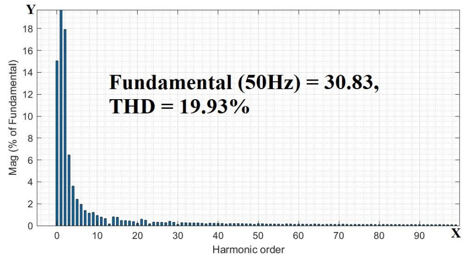

***Fig. 13**: FFT analysis under dynamic with sag swell without controller.*

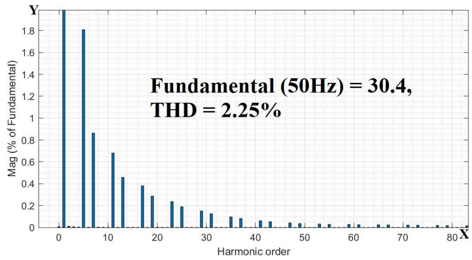

***Fig. 14**: FFT analysis under dynamic with sag swell with controller.*

THD levels can be decreased by the ANFIS controller to less than 2% after compensation.

5.6 Distorted grid voltage condition

In this condition, I have injected the harmonics in the grid voltages manually to check the proposed controller's robustness. In this condition, the performance of the proposed controller is found well and the THD analysis is within the limits which is observed from Fig. 21.

6. COMPARATIVE ANALYSIS

Tables 3 and 4 compare the suggested method to the employed PLL, grid synchronization, THD, sampling time, accuracy, types of filter settling time, amplitude tracking, complexity, and DC offset rejection techniques. This technique is demonstrated, and it is discovered that its performance in steady state and other conditions is the best of all of these techniques. Table 2 shows the

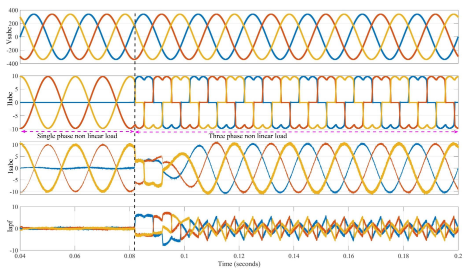

***Fig. 15**: Load removed.*

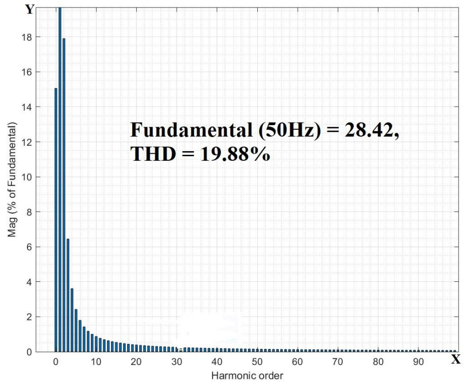

***Fig. 16**: FFT analysis under single-phase dynamic load without controller.*

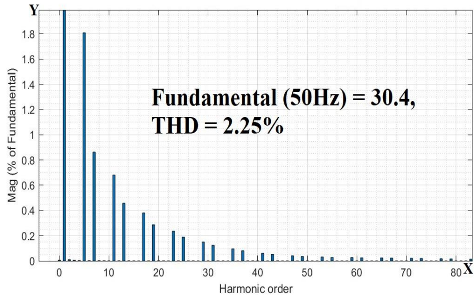

***Fig. 17**: FFT analysis under single-phase dynamic load with controller.*

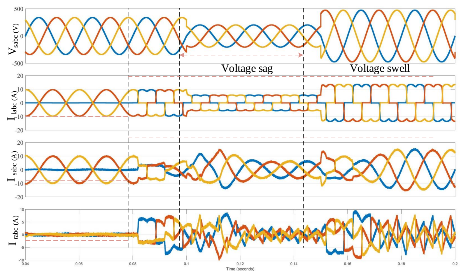

***Fig. 18**: Load removed with swag and swell.*

grid current's harmonic analysis. However, the source current THD using the suggested technique is lower than that of adaptive methods. When compared to other controllers, it is discovered that the one being presented is superior.

7. CONCLUSION

This documentation covered the simulation, modelling, and control of a PV and wind hybrid power system that is connected to the grid. The system is simulated in the MATLAB/Simulink environment. A wind turbine based on a PMSG is used in a wind energy conversion system. A rectifier is used to convert the wind and PV outputs to dc before being fed into an inverter, which

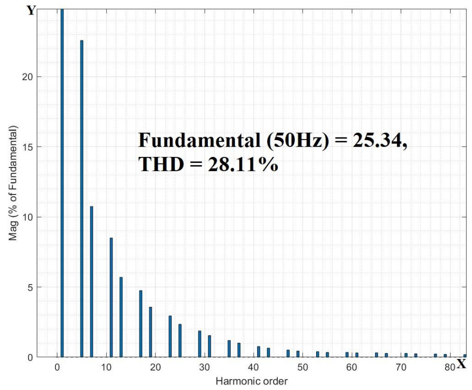

Fig. 19: *FFT analysis under single phase nonlinear load sag and swell without controller.*

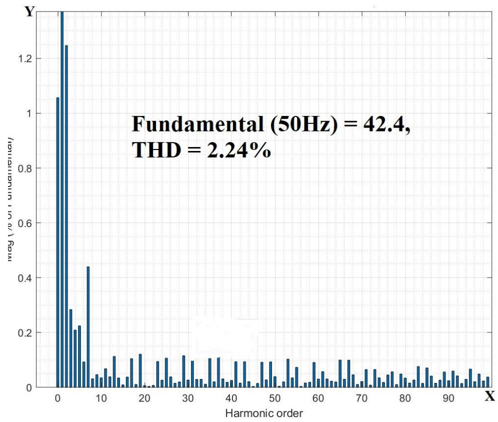

Fig. 20: *FFT analysis under single-phase nonlinear load sag and swell with controller.*

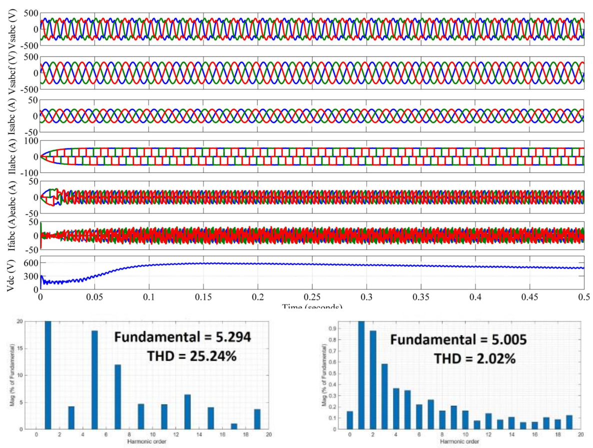

Fig. 21: *Grid voltages distorted condition.*

then feeds the combined wind and PV output to the grid. The system characteristics, harmonics, long-term voltage disturbances, short-term voltage imbalances, and modified p-q theory based on ANFIS were all taken into account by the ANFIS controller.

REFERENCES

[1] N. Babu P, J. M. Guerrero, P. Siano, R. Peesapati and G. Panda, "An Improved Adaptive Control Strategy in Grid-Tied PV System With Active Power Filter for Power Quality Enhancement," in *IEEE Systems Journal*, vol. 15, no. 2, pp. 2859-2870, June 2021.

[2] PN Babu, Bhabani Kumari Choudhury, Biswajit Kar, and Biswajit Halder, "Modelling of a hybrid active power filter for power quality improvement using synchronous reference frame theory" in *International Journal of Engineering Research & Technology*, vol. 6, no. 3, pp. 369–374, 2017

[3] P Narendra Babu, Biwajit Kar, and Biswajit Halder, "Modelling and analysis of a hybrid active power filter for power quality improvement using hysteresis current control technique" in *2016 7th India International Conference on Power Electronics (IICPE)*, pages 1–6. IEEE, 2016.

[4] Adel Merabet, Khandker Tawfique Ahmed, Hussein Ibrahim, Rachid Beguenane, and Amer MYM Ghias, "Energy management and control system for laboratory scale microgrid based wind-pv-battery" in *IEEE transactions on sustainable energy*, vol. 8, no. 1, pp. 145–154, 2016.

[5] Narendra Babu, Ranga Babu Peesapati, and Gayadhar Panda, "An adaptive current control technique in grid-tied pv system with active power filter for power quality improvement" in *TENCON 2019-2019 IEEE Region 10 Conference (TENCON)*, pages 187-191. IEEE, 2019

[6] Mallala B. Upendar Srimatha, S, "A novel ANFIS controlled customized UPQC device for power quality enhancement" in *Journal of Electrical Systems and Inf. Technol.*, Vol. 10, no. 55, 2024.

[7] Narendra Babu Perumallapalli, Baladhandautham Chitti Babu, Rangababu Peesapati, and Gayadhar Panda, "Three-phase grid-tied photovoltaic system with an adaptive current control scheme in active power filter, in *Energy Sources, Part A: Recovery, Utilization, and Environmental Effects*, pages 1–25, 2020.

[8] P Narendra Babu, Ranga Babu Peesapati, and Gayadhar Panda, "A pre-filtering based current control strategy in grid-tied photovoltaic systems with active power filter for harmonic mitigation", in *TENCON 2019-2019 IEEE Region 10 Conference (TENCON)*, pages 1003-1008. IEEE, 2019.

[9] P. N. Babu, P. R. Babu, B. Chittibabu and G. Panda, "Three-Phase Grid-tied Photovoltaic System with an Adaptive Current Control Scheme in Active Power Filter," in *2019 IEEE 1st International Conference on Energy, Systems and Information Processing (ICESIP)*, Chennai, India, 2019, pp. 1-6.

[10] Imad Aboudrar, Soumia El Hani, Mohamed Saleck Heyine, and Nisrine Naseri, "Dynamic modeling and robust control by adrc of grid-connected hybrid pv-wind energy conversion system," in

Mathematical Problems in Engineering, 2019, pp. 1-19, 2019.

[11] T. S. V. S. P. Teja, S. K. Prince, M. R, D. Adhikari, N. B. P and G. Panda, "Enhancement of Power Quality with a Wind-Integrated Shunt Active Power Filter," in *2022 4th International Conference on Energy, Power and Environment (ICEPE)*, Shillong, India, 2022, pp. 1-6.

[12] V. N. Kumar, N. Babu P., R. Kiranmayi, P. Siano and G. Panda, "Improved Power Quality in a Solar PV Plant Integrated Utility Grid by Employing a Novel Adaptive Current Regulator," in *IEEE Systems Journal*, vol. 14, no. 3, pp. 4308-4319, Sept. 2020.

[13] Kaushal, Jitender and Basak, Prasenjit, "Power quality control based on voltage sag/swell, unbalancing, frequency, THD and power factor using artificial neural network in PV integrated AC microgrid," in *Sustainable Energy, Grids and Networks*, vol. 23, pp. 100365, Elsevier, 2020.

[14] Mohammad Amir, Anjani Kumar Prajapati, and Shady S Refaat, "Dynamic performance evaluation of grid-connected hybrid renewable energy-based power generation for stability and power quality enhancement in smart grid," in *Frontiers in Energy Research*, vol. 10, pp. 222, 2022.

[15] Azoug, Hakim and Belmili, Hocine and Bouazza, Fekkak, "Grid-connected control of PV-Wind hybrid energy system," in *International Journal of Power Electronics and Drive Systems*, vol. 12, no. 2, pp. 1228, 2021.

[16] Neeraj Priyadarshi, Sanjeevikumar Padmanaban, Mahajan Sagar Bhaskar, Frede Blaabjerg, and Amarjeet Sharma, "Fuzzy svpwm- based inverter control realisation of grid integrated photovoltaic-wind system with fuzzy particle swarm optimisation maximum power point tracking algorithm for a grid-connected pv/wind power generation system: hardware implementation," in *IET Electric Power Applications*, vol. 12, no. 7, pp. 962-971, 2018

[17] Narendra Babu P, "Adaptive grid-connected inverter control schemes for power quality enrichment in microgrid systems: Past, present, and future perspectives", in *Electric Power Systems Research*, vol. 230, pp. 110288, 2024, DOI: 10.1016/j.epsr.2024.110288

[18] FE Tahiri, K Chikh, and M Khafallah, "Optimal management energy system and control strategies for isolated hybrid solar-wind-battery-diesel power system," in *Emerging Science Journal*, vol. 5, no. 2, pp. 111-124, 2021

[19] A. F. Tazay, A. M. A. Ibrahim, O. Noureldeen and I. Hamdan, "Modeling, Control, and Performance Evaluation of Grid-Tied Hybrid PV/Wind Power Generation System: Case Study of Gabel El-Zeit Region, Egypt," in *IEEE Access*, vol. 8, pp. 96528-96542, 2020.

[20] Hamdan, I and Ibrahim, Ahmed MA and Noureldeen, Omar, "Modified STATCOM control strategy for fault ride-through capability enhancement of grid-connected PV/wind hybrid power system during voltage sag," in *SN Applied Sciences*, vol. 2, pp. 1-19, springer, 2020.

[21] Narendra P Babu, Chitti B Babu, Ranga Babu Peesapati, and Gayadhar Panda, "An optimal current control scheme in grid-tied hybrid energy system with active power filter for harmonic mitigation," in *International Transactions on Electrical and Energy Systems*, vol. 30, no. 3, 2020.

[22] B. Mangu, S. Akshatha, D. Suryanarayana and B. G. Fernandes, "Grid-Connected PV-Wind-Battery-Based Multi-Input Transformer-Coupled Bidirectional DC-DC Converter for Household Applications," in *IEEE Journal of Emerging and Selected Topics in Power Electronics*, vol. 4, no. 3, pp. 1086-1095, Sept. 2016.

[23] Patil, Mr Anantrao V and Mulla, Anwar M and Patil, Mr Swapnil D and Jadhav, Mr Ajit B, "Power Quality Improvement in a Grid-connected Renewable Energy System" in *Open Access Repository*, vol. 9, no. 7, pp. 7-15, 2022.

[24] Jha, Kanchan and Shaik, Abdul Gafoor, "A comprehensive review of power quality mitigation in the scenario of solar PV integration into utility grid", in *e-Prime-Advances in Electrical Engineering, Electronics and Energy*, pp. 100103, Elsevier, 2023.

[25] P. N. Babu, P. R. Bana, R. B. Peesapati and G. Panda, "An Interleaved Buck Converter Based Active Power Filter for Photovoltaic Energy Application," in *2019 International Conference on Power Electronics Applications and Technology in Present Energy Scenario (PETPES)*, Mangalore, India, 2019, pp. 1-6.

[26] S. J. Pinto, N. B. P, R. Peesapati and G. Panda, "Monitoring and Control of MultiBus Microgrid System Using FPGA Platform," in *2019 IEEE Region 10 Symposium (TENSYMP)*, Kolkata, India, 2019, pp. 260-265.

[27] P et. al., "A novel adaptive fuzzy-based controller design using field programmable gate arrays for grid-connected photovoltaic systems,", in *Advances in Smart Grid Power System, Academic Press*, pp. 331-364, ISBN 9780128243374.

[28] K. P. Panda, N. B. P, S. K. Bisoyi and G. Panda, "Reduced Switch Quadruple Boost Switched-Capacitor based Multilevel Inverter," 2020 3rd International Conference on Energy, Power and Environment: Towards Clean Energy Technologies, Shillong, Meghalaya, India, 2021, pp. 1-6.

Narendra Babu P received the Ph.D. and M.Tech degrees in electrical engineering department with power and energy systems specialization from the National Institute of Technology Meghalaya, Shillong, in 2017 and 2022, respectively. He received the B.Tech. degree in electrical and electronics engineering from Jawaharlal Nehru Technological University Hyderabad, Hyderabad, India. Presently, he is working as an assistant professor at the school of EEE, VIT Bhopal University since 2021. He has as a research experience of 4 years as a Senior Research Fellow/Project Associate with RECTPCL-CSR Funded Project during 2017-2021, Department of Electrical Engineering, National Institute of Technology Meghalaya. He has as an industry experience of 5 years as an assistant electrical engineer during 2010-2015. He has published more than 30 research publications in IEEE Transactions/Journals, international conferences and book chapters. He received more than 460 Google Scholar citations with 11 h-index and 13 i-10 index. He is a reviewer of several IEEE Transactions, IET, Wiley, Taylor & Francis and other SCI Journals. He is working as an associate editor in several journals. His current research interests include renewable energy technologies, hybrid ac–dc Microgrid, power quality, adaptive control, Solar PV system, power management, and control of grid-tied inverters.